

Phosphinoalkylsilyl Complexes. 12. Stereochemistry of the Tridentate Bis(diphenylphosphinopropyl)silyl (biPSi) Framework: Complexation That Introduces “Face Discrimination” at Coordinatively Unsaturated Metal Centers. X-ray Crystal and Molecular Structures of Pt[SiMe(CH₂CH₂CH₂PPh₂)₂]Cl, IrH[SiMe(CH₂CH₂CH₂PPh₂)₂]Cl, and RuH[SiMe(CH₂CH₂CH₂PPh₂)₂](CO)₂¹

Ron D. Brost, Gregg C. Bruce, Frederick L. Joslin, and Stephen R. Stobart*[†]

Department of Chemistry, Auburn University, Auburn, Alabama 36849

Received June 19, 1997[⊗]

Reaction of the bis(phosphinoalkyl)silanes RSiH[(CH₂)_nPR¹]₂ (R = Me or Ph, *n* = 2 or 3, R¹ = Ph or Cy, *i.e.*, cyclohexyl; biPSiH for R = Me, *n* = 2, R¹ = Ph) with Pt(COD)Cl₂ (COD = cycloocta-1,5-diene), [Ir(COD)Cl]₂, *trans*-M(PPh₃)₂(CO)Cl (M = Rh or Ir), or Ru₃(CO)₁₂ affords products that are complexes of tridentate biPSi silyl analogues, in which the Si center is anchored through attachment of *trans* P atoms at the transition-metal site. The platinum(II) compounds Pt[SiMe(CH₂CH₂PPh₂)₂]Cl (**1**), Pt[SiMe(CH₂CH₂PCy₂)₂]Cl (**2**), Pt[SiPh(CH₂CH₂PCy₂)₂]Cl (**3**), Pt[SiPh(CH₂CH₂PPh₂)(CH₂CH₂PCy₂)]Cl (**4**), Pt[SiMe(CH₂CH₂-CH₂PPh₂)₂]Cl (**5**), Pt[SiMe(CH₂CH₂CH₂PCy₂)₂]Cl (**6**), and Pt[SiPh(CH₂CH₂CH₂PPh₂)₂]Cl (**7**), which have been characterized by ¹H, ¹³C, and ³¹P NMR spectroscopy, possess distinguishable square faces with Me on Si projecting in one direction and the buckled (CH₂)_n backbones in the other. Cleavage of the Pt–Si bond in Pt(biPSi)Cl (**5**) by HCl affords a pair of diastereomers HPt[(PPh₂CH₂CH₂CH₂)₂Si(Cl)Me]Cl (**8,8'**) in which the two P atoms are also *trans*. The five-coordinate, 16e, d⁶ Ir(III) complex IrH(biPSi)Cl (**9**) is isolated as a single diastereomer, but octahedral IrH(biPSi)(CO)Cl is formed as a 3:1 mixture of stereoisomers (**10** and **11**, CO or Cl *trans* to Si, respectively, *i.e.*, H *trans* to Cl or CO) that react with SnCl₂ to afford (also 3:1) the analogues IrH(biPSi)(CO)SnCl₃ (**12** and **13**). Treatment of **10** and **11** (3:1) with LiAlH₄ yields a diastereomeric pair of *cis*-dihydrido complexes IrH₂(biPSi)(CO) (**14,14'**) (1:3), accompanied by a *trans*-dihydrido stereoisomer **15** and a *fac*-biPSi stereoisomer **16** as minor products; in **14, 14'** and **15** the hydride ligands are nonequivalent and show ²J_{HH*cis* = 5.1, 4.4 Hz, ²J_{HH*trans* ≈ 0, respectively. Similar treatment with LiAl²H₄ affords monodeuterioisotopomers **14a,14'a**, while reaction of compound **9** with LiAlH₄ under CO gas initially affords **16** as a single product that subsequently isomerizes to **14,14'**. The octahedral, 18e, d⁶ Ru(II) homologues RuH[SiMe(CH₂CH₂PPh₂)₂](CO)₂ (**17**) and RuH(biPSi)(CO)₂ (**18**) are formed in sealed-tube reactions at elevated temperature but in very poor yields. NMR spectroscopy suggests that in solution the biPSi backbones of **2–7** and **9–13** are equivalent, establishing planar symmetry (point group C_s) perpendicular to the ligand template, although this is not maintained in the solid state as shown crystallographically for compounds **5, 9, 13**, and **18**. Bond distances *trans* to Si are long in **5** and **13** (2.44 and 2.66 Å, to Cl or SnCl₃, respectively), but in **9** Ir–Cl at 2.30 Å is short, occupying the equatorial plane with Si and H in a distorted TBP structure (Si–Ir–Cl 129°). The M–Si distances are 2.31 (**5**), 2.29 (**9**), 2.42 (**13**), and 2.46 Å (**18**). In **9** and **13**, the H at Ir is *anti* vs Me on Si (of biPSi), whereas in **18**, the Ir–H and Si–Me bonds are *syn*.}}

Introduction

Selectivity in cycles that are catalyzed by soluble transition-metal complexes is accountable for² not only, in terms of shape recognition of substrate by coordina-

tion geometry^{3,4} but may depend also on possible changes in electron availability at the active metal site

[†] Current address: Department of Chemistry, University of Victoria, British Columbia, Canada V8W 2Y2.

[⊗] Abstract published in *Advance ACS Abstracts*, November 15, 1997.
(1) Part 11: Auburn, M. J.; Holmes-Smith, R. D.; Stobart, S. R.; Bakshi, P. K.; Cameron, T. S. *Organometallics* **1996**, *15*, 3032.

(2) Quan, R. W.; Li, Z.; Jacobsen, E. N. *J. Am. Chem. Soc.* **1996**, *117*, 8156.

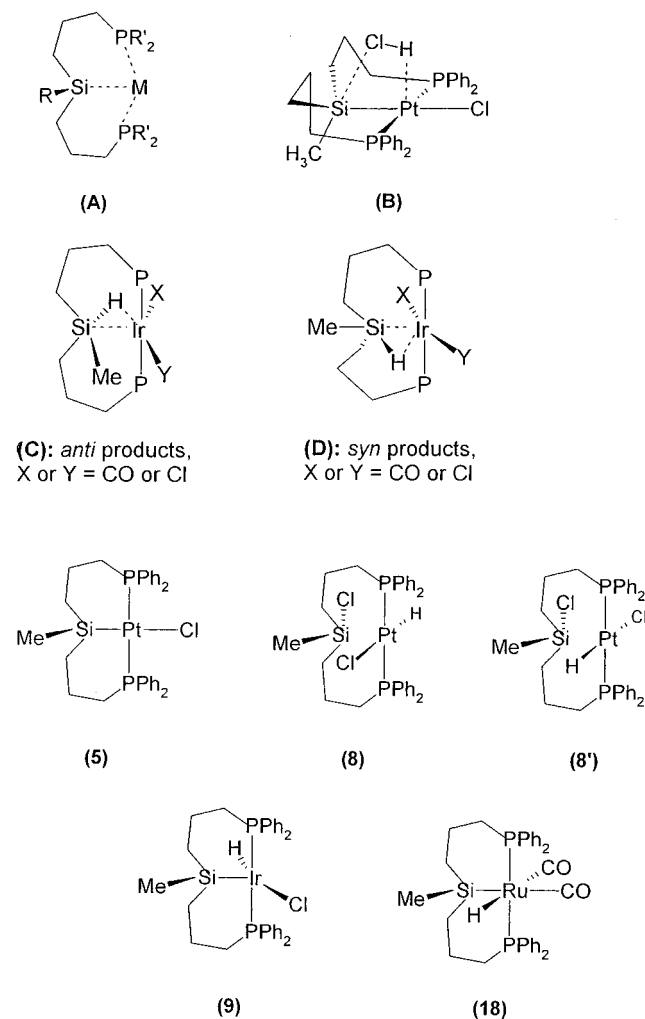
(3) Barnhart, R. W.; Wang, X.; Noheda, P.; Bergens, S. H.; Whelan, J.; Bosnich, B. *J. Am. Chem. Soc.* **1994**, *116*, 1721.

(4) (a) Halpern, J. In *Asymmetric Synthesis*; Morrison, J. D., Ed.; Academic Press: New York, 1985; Vol. 5, pp 41–69. (b) Brown, J. M. In *Homogeneous Catalysis with Metal-Phosphine Complexes*; Pignolet, L. H., Ed.; Plenum: New York, 1983; pp 137. (c) Landis, C. R.; Halpern, J. *J. Am. Chem. Soc.* **1987**, *109*, 1746. (d) Brown, J. M.; Evans, P. L. *Tetrahedron* **1988**, *44*, 4905. (e) Bosnich, B. *Pure Appl. Chem.* **1990**, *62*, 1131. (f) Bogdan, P. L.; Irwin, J. J.; Bosnich, B. *Organometallics* **1989**, *8*, 1450. (g) Giovannetti, J. S.; Kelly, C. M.; Landis, C. R. *J. Am. Chem. Soc.* **1993**, *115*, 4040.

that result directly from^{5–7} chemical modification of the ligand framework. Such dependence is identified explicitly in the theoretical modeling of associative dihydrogen approach to a coordinatively unsaturated d⁸ center,⁸ which has been shown to be controlled primarily by electronic factors that include competing ligand *trans* influences. We have been seeking to determine if the electron-releasing properties and strong *trans* influence of silyl ligands⁹ may alter or enhance the catalytic performance of soluble platinum-group metal centers in hydrogenation, hydroformylation, or hydrosilylation reactions. Investigation of this possibility necessitates chelate attachment as a means for suppressing silyl elimination, which is otherwise facile, a requirement that has been met¹⁰ by using polydentate phosphinoalkylsilyl (PSi) ligands for simultaneous binding through Si and P (see A).

In the hierarchy of ligand electronic effects, exceptionally strong σ -donor character is attributed to silyl complexation because it has a remarkable impact¹¹ on the parameters that provide a measure of the relative *trans*-influencing capacity. In these terms, $-\text{SiR}_3$ exceeds both $-\text{H}$ and $-\text{CH}_3$ (as is shown convincingly by crystallographic data provided below as well as data recently^{12,13} reported); this empirical order is again supported by contemporary theoretical arguments^{8,14,15} (based *inter alia* on Taft parameters) that identify σ -donor ability as the dominant force (*vs* much weaker π -donation) in *trans* atom or group labilization. By directing the electronic labilizing character of silyl complexation within the sterically controlled environment of a supporting framework, polydentate PSi ligand attachment should be capable of exerting an unusually powerful organizing effect over bond formation by other atoms at the same metal center. Accordingly, complexes so formed are strongly regioselective homogeneous hydroformylation catalysts.¹⁶ Simple chelation, using the analogue $\text{Ph}_2\text{PCH}_2\text{CH}_2\text{SiMe}_2-$ (chel) of diphos ($\text{Ph}_2\text{PCH}_2\text{CH}_2\text{PPh}_2$), minimizes the steric impact of PSi ligation;^{10,17} while encapsulation of the reactive site in a tetradentate cage by $[\text{Ph}_2\text{PCH}_2\text{CH}_2\text{CH}_2]_3\text{Si}-$ (triPSi)

appears to be too restricting¹⁸ and shuts down catalysis.^{16,19} As shown below, however, the stereochemistry of tridentate $[\text{Ph}_2\text{PCH}_2\text{CH}_2\text{CH}_2]_2\text{SiMe}-$ (biPSi) attachment (see A and B) develops distinguishable molecular faces at an unsaturated metal center,¹⁶ a property that is not common²⁰ and will direct diastereoselective substrate entry into a position *trans* to Si. A five-



(5) Jacobsen, E. N.; Zhang, W.; Güler, M. L. *J. Am. Chem. Soc.* **1991**, *113*, 6703.

(6) Bender, B. R.; Koller, M.; Nanz, D.; von Philipsborn, W. *J. Am. Chem. Soc.* **1993**, *115*, 5889. See also: Tedesco, V.; von Philipsborn, W. *Organometallics* **1995**, *14*, 3600.

(7) Schnyder, A.; Togni, A.; Wiesli, U. *Organometallics* **1997**, *16*, 255.

(8) Burk, M. J.; McGrath, M. P.; Wheeler, R.; Crabtree, R. H. *J. Am. Chem. Soc.* **1988**, *110*, 5034. Sargent, A. L.; Hall, M. B.; Guest, M. F. *J. Am. Chem. Soc.* **1992**, *114*, 517. Sargent, A. L.; Hall, M. B. *Inorg. Chem.* **1992**, *31*, 317.

(9) (a) Auburn, M. J.; Stobart, S. R. *Inorg. Chem.* **1985**, *24*, 317. (b) Auburn, M. J.; Holmes-Smith, R. D.; Stobart, S. R. *J. Am. Chem. Soc.* **1984**, *106*, 1314.

(10) (a) Holmes-Smith, R. D.; Stobart, S. R.; Cameron, T. S.; Jochem, K. *J. Chem. Soc., Chem. Commun.* **1981**, 937. (b) Grundy, S. L.; Holmes-Smith, R. D.; Stobart, S. R.; Williams, M. A. *Inorg. Chem.* **1991**, *30*, 3333.

(11) (a) Heaton, B. T.; Pidcock, A. *J. Organomet. Chem.* **1968**, *14*, 235. (b) Appleton, T. G.; Clark, H. C.; Manzer, L. E. *Coord. Chem. Rev.* **1973**, *10*, 335.

(12) Kapoor, P.; Lövsqvist, K.; Oskarsson, Å. *Acta Crystallogr.* **1995**, *C51*, 611.

(13) Aizenberg, M.; Milstein, D. *J. Am. Chem. Soc.* **1995**, *117*, 6456.

(14) Abu-Hasanayn, F.; Krogh-Jespersen, K.; Goldman, A. S. *Inorg. Chem.* **1993**, *32*, 495.

(15) Lichtenberger, D. L.; Rai-Chaudhuri, A. *J. Am. Chem. Soc.* **1991**, *113*, 2923.

(16) Stobart, S. R.; Grundy, S. L.; Joslin, F. L. U.S. Patent 4,950,798, 1990; Canadian Patent 1,327,365, 1994.

(17) Cameron, T. S.; Holmes-Smith, R. D.; Jochem, K.; Stobart, S. R.; Vefghi, R.; Zaworotko, M. J. *J. Chem. Soc. Dalton Trans.* **1987**, 969.

coordinate iridium(III) complex (16 electron, d⁶) of this type, $\text{IrH}(\text{biPSi})\text{Cl}$, is crystallographically shown to be another example of the hitherto rare dist-TBP geometry that was first recognized¹ by us, Werner, and Fryzuk and has subsequently been rationalized²¹ using molecular orbital arguments by Eisenstein, Caulton *et al.*

In addition we have found that related "face-discrimination" in a coordinatively saturated, six-coordinate, 18-electron dihydrido-iridium(III) analogue $\text{IrH}_2(\text{biPSi})(\text{CO})$ also leads to the existence of diastereomers in which one H at Ir is either *syn* or *anti* *vs* the methyl

(18) Joslin, F. L.; Stobart, S. R. *J. Chem. Soc., Chem. Commun.* **1989**, 504.

(19) Hendricksen, D. E.; Oswald, A. E.; Ansell, G. B.; Leta, S.; Kastrop, R. V. *Organometallics* **1989**, *8*, 1153.

(20) (a) Fryzuk, M. D.; MacNeil, P. A.; Rettig, S. J. *J. Am. Chem. Soc.* **1985**, *107*, 6708. (b) Yang, C.; Socol, S. M.; Kountz, D. J.; Meek, D. W. *Inorg. Chim. Acta* **1986**, *114*, 119. (c) Bautista, M. T.; Earl, K. A.; Maltby, P. A.; Morris, R. H. *J. Am. Chem. Soc.* **1988**, *110*, 4056.

(21) (a) Riehl, R.-F.; Jean, Y.; Eisenstein, O.; Pélissier, M. *Organometallics* **1992**, *11*, 729. (b) Albinati, A.; Bakmutov, V. I.; Caulton, K. G.; Clot, E.; Eckert, J.; Eisenstein, O.; Gusev, D. G.; Grushin, V. V.; Hauger, B. E.; Klooster, W. T.; Koetzle, T. F.; McMullan, R. K.; O'Loughlin, T. J.; Pelissier, M.; Ricci, R. S.; Sigalas, M. P.; Vymontis, A. B. *J. Am. Chem. Soc.* **1993**, *115*, 7300.

substituent at Si (also bonded to Ir, see **A**). These products are rare examples of transition-metal complexes in which two hydride ligands are nonequivalent, resulting in the resolution of $^2J_{\text{HH}(cis)}$ (~ 5 Hz) but not of the corresponding *trans* coupling ($J \approx 0$) in ^1H NMR spectra at ambient temperature.

Experimental Section

Full details of general synthetic procedures, protocol for instrumental measurements, analytical techniques, and methodology used for access to transition-metal precursors have been given in earlier papers.^{9,10,17} Bis(diorganophosphinoalkyl)organosilane (biPSiH) synthesis has also been described elsewhere:²² these air-sensitive ligand precursors were manipulated by using syringe techniques under standard inert-atmosphere conditions.

Synthesis of biPSi Complexes. A. Of Platinum(II). **i. Pt[SiMe(CH₂CH₂PPh₂)₂]Cl (1).** Dropwise addition of a solution of MeSiH(CH₂CH₂PPh₂)₂ (99 mg, 0.21 mmol) in dry THF (5 mL) to a solution of [Pt(COD)Cl₂] (79 mg, 0.21 mmol) in a mixture of THF (7 mL) and NEt₃ (1 mL) resulted in rapid formation of a white precipitate. Removal of the volatiles left solid material, which after thorough washing left the product (124 mg, 84%), which proved to be insoluble in benzene, CH₂Cl₂, Et₂O, THF, acetone, DMF, or water. Anal. Calcd for C₂₉H₃₁ClP₂PtSi: C, 49.75; H, 4.46. Found: C, 50.02; H, 4.59.

ii. Pt[SiMe(CH₂CH₂PCy₂)₂]Cl (2). Dry benzene (10 mL) and NEt₃ (1 mL) were added to MeSiH(CH₂CH₂PCy₂)₂ (0.20 g, 0.41 mmol). Rapid addition of this mixture to a stirred slurry of [Pt(COD)Cl₂] (0.15 g, 0.41 mmol) in benzene (10 mL) resulted in immediate dissolution of the solids to give a slightly turbid solution. Removal of the volatiles *in vacuo* left a sticky solid which was extracted with benzene (5 mL). Removal of the latter followed by two successive similar extraction and evaporation cycles afforded the pure product (0.25 g, 84%). Anal. Calcd for C₂₉H₅₅ClP₂PtSi: C, 48.09; H, 7.65. Found: C, 48.09; H, 7.62.

iii. Pt[SiPh(CH₂CH₂PCy₂)₂]Cl (3). A procedure analogous to that used to obtain complex **2** was followed: a solution in benzene (10 mL) of PhSiH(CH₂CH₂PCy₂)₂ (0.15 g, 0.28 mmol) was run into a slurry of [Pt(COD)Cl₂] (0.10 g, 0.28 mmol) also in benzene (10 mL), and NEt₃ (1 mL) was immediately added with vigorous stirring. After 10 min, removal of the volatiles *in vacuo* followed by extraction of the solid residue with benzene (2 × 10 mL) afforded the product as an off-white solid (0.08 g, 35%). Anal. Calcd for C₃₄H₅₇ClP₂PtSi: C, 51.93; H, 7.31. Found: C, 52.01; H, 6.93.

iv. Pt[SiPh(CH₂CH₂PPh₂)(CH₂CH₂PCy₂)]Cl (4). In a similar manner to that described in **A.iii**, PhSiH(CH₂CH₂PCy₂)(CH₂CH₂Ph₂) (0.11 g, 0.21 mmol) and [Pt(COD)Cl₂] (0.08 g, 0.21 mmol) were allowed to react in benzene (10 mL) in the presence of NEt₃ (1 mL). Recovery by extraction into benzene afforded the product, an off-white solid (0.12 g, 75%). Anal. Calcd for C₃₄H₄₅ClP₂PtSi: C, 52.70; H, 5.86. Found: C, 52.18; H, 5.62.

v. Pt[SiMe(CH₂CH₂CH₂PPh₂)₂]Cl (5). After reaction of MeSiH(CH₂CH₂CH₂PPh₂)₂ (0.50 g, 1.00 mmol) with [Pt(COD)Cl₂] (0.37 g, 1.00 mmol) also in benzene (10 mL) with NEt₃ (1 mL), the cream-colored solid product was recovered as described before (0.53 g, 73%). Anal. Calcd for C₃₁H₃₅ClP₂PtSi: C, 51.13; H, 4.85. Found: C, 50.99; H, 4.81. Crystals suitable for X-ray diffraction were obtained by slow evaporation in air of a saturated solution of the complex in diethyl ether.

vi. Pt[SiMe(CH₂CH₂CH₂PCy₂)₂]Cl (6). Reaction of MeSiH(CH₂CH₂CH₂PCy₂)₂ (0.18 g, 0.35 mmol) with [Pt(COD)Cl₂] (0.13 g, 0.35 mmol) in benzene solution with NEt₃ as in **A.v** afforded the cream-colored solid product (0.20 g, 76%).

Anal. Calcd for C₃₁H₅₉ClP₂PtSi: C, 49.49; H, 7.91. Found: C, 49.07; H, 7.72.

vii. Pt[SiPh(CH₂CH₂CH₂PPh₂)₂]Cl (7). Similar treatment of PhSiH(CH₂CH₂CH₂PPh₂)₂ (0.30 g, 0.53 mmol) with [Pt(COD)Cl₂] (0.20 g, 0.53 mmol) in benzene solution with NEt₃ yielded another cream-colored product (0.30 g, 72%). Anal. Calcd for C₃₆H₃₇ClP₂PtSi: C, 54.71; H, 4.72. Found: C, 54.72; H, 4.95.

viii. Diastereoisomeric Complexes PtH[(PPh₂CH₂CH₂CH₂)₂Si(Cl)Me]Cl (8,8'). Compound **5** (40 mg, 0.06 mmol) was dissolved in a mixture of THF (5 mL) and methanol (1 mL), then acetyl chloride (5 mg, 0.06 mmol) in THF was added. After the mixture was stirred (5 min), removal of the volatiles left a white solid product (38 mg, 91%), shown by NMR to be a mixture of diastereomers. Anal. Calcd for C₃₁H₃₆Cl₂P₂PtSi: C, 48.69; H, 4.57. Found: C, 48.21; H, 4.55.

B. Complexes of Iridium(III). **i. IrH[SiMe(CH₂CH₂CH₂PPh₂)₂]Cl (9).** Solutions in benzene (10 mL) of MeSiH(CH₂CH₂CH₂PPh₂)₂ (0.12 g, 0.24 mmol) and [Ir(COD)Cl]₂ (0.08 g, 0.12 mmol) were mixed and then stirred at ambient temperature. After 150 min, the solvent was removed *in vacuo*, leaving behind the product as a yellow powder (0.16 g, 95%). Anal. Calcd for C₃₁H₃₆ClIrP₂Si: C, 51.26; H, 4.99. Found: C, 51.46; H, 4.99. During refrigeration at -20 °C, a solution of the pure complex in an ether/hexane mixture slowly deposited shiny orange crystals that were suitable for X-ray diffraction.

ii. Isomeric Complexes IrH[SiMe(CH₂CH₂CH₂PPh₂)₂](CO)Cl (10 and 11). When solutions in CH₂Cl₂ (10 mL) of MeSiH(CH₂CH₂CH₂PPh₂)₂ (0.36 g, 0.73 mmol) and *trans*-[Ir(PPh₃)₂(CO)Cl] (0.57 g, 0.73 mmol) were stirred together, the initially cloudy yellow mixture became clear and colorless. Evaporation of the solvent left a sticky white solid that was washed thoroughly with Et₂O to afford the product as a fine white powder (0.36 g, 66%), which was shown by NMR to be a mixture of two isomers in a 3:1 ratio. Anal. Calcd for C₃₂H₃₆ClIrOP₂Si, mono-CH₂Cl₂ solvate: C, 47.22; H, 4.56. Found: C, 47.18; H, 5.06.

iii. Isomeric Complexes IrH[SiMe(CH₂CH₂CH₂PPh₂)₂](CO)(SnCl₃) (12 and 13). The mixture of isomers **10** and **11** (80 mg, 0.11 mmol) and anhydrous SnCl₂ (20 mg, 0.11 mmol) were dissolved together in THF (10 mL) and then stirred for 60 min. Removal of the solvent left a white, powdery product (100 mg, 100%), shown by NMR to be a mixture of isomers, again in a 3:1 ratio. Anal. Calcd for C₃₂H₃₆Cl₃IrOP₂SiSn: C, 40.72; H, 3.84. Found: C, 40.38; H, 3.62.

iv. Isomeric Complexes IrH₂[SiMe(CH₂CH₂CH₂PPh₂)₂](CO) (14, 15, and 16). The mixture of isomers **10** and **11** (0.11 g, 0.14 mmol) was dissolved in THF (10 mL), then excess LiAlH₄ in THF was slowly added, leading to the formation of a yellow-grey suspension. After removal of the volatiles, the residue was extracted with toluene (3 × 5 mL) and then the extracts were filtered through a plug of nonabsorbent cotton. Evaporation of the solvent yielded the off-white product (0.05 g, 52%), which was shown by NMR to consist mainly (*ca.* 84%) of a mixture of a pair of diastereoisomers in a 3:1 ratio (*i.e.*, **14** and **14'**) together with a minor proportion of two other isomers (**15** and **16**). Anal. Calcd for C₃₂H₃₇IrOP₂Si: C, 53.39; H, 5.18. Found: C, 53.01; H, 5.03.

C. Complexes of Ruthenium(II). **i. RuH[SiMe(CH₂CH₂CH₂PPh₂)₂](CO)₂ (17).** The precursor MeSiH(CH₂CH₂CH₂PPh₂)₂ (0.21 g, 0.47 mmol) dissolved in a 50/50 mixture of hexanes/THF (18 mL) was added to solid Ru₃(CO)₁₂ (0.09 g, 0.14 mmol) in a Carius tube, which was sealed then heated at 140 °C for 8 h in the dark. After this time the initially orange solution had become bright yellow, and on cooling a yellow solid deposited on the walls of the tube. This material was collected (*ca.* 15% yield) following decantation of the supernatant, but evaporation of the latter left a sticky residue from which no more of the product could be isolated. Anal. Calcd for C₃₁H₃₂O₂P₂RuSi: C, 59.31; H, 5.14. Found: C, 59.20; H, 4.97. No reaction was observed even after prolonged periods

(22) (a) Holmes-Smith, R. D.; Osei, R. D.; Stobart, S. R. *J. Chem. Soc., Perkin Trans. 1* **1983**, 861. (b) Joslin, F. L.; Stobart, S. R. *Inorg. Chem.* **1993**, *32*, 2221.

Table 1. Carbon-13 and Phosphorus-31 NMR Data^a

compd	$\delta(\text{PR}_2)^b$	$\delta\Delta^c$	$\delta(\text{SiR})^d$	$\delta(\text{SiCH}_2)$	$\delta(\text{PCH}_2\text{CH}_2)^e$	$\delta(\text{PCH}_2)$
2	63.3 (2981)	+61.2	-0.9 (66)			19.6 (120; ^f 16 ^g)
3	61.9 (2903)	+58.0	141 (51)	16.6 (9 ^h)		20.3 (16 ^g)
4	44.9 (2952)	+58.6	140 (49)	8.0 (n.o.)		14.3 (102; ^f 18 ^g)
	62.5 (2855)	+54.5	15.6 (118; ^f 17 ^h)		19.7 (125; ^f 33 ^g)	
5	8.6 (2825)	+25.3	3.6 (75)	16.6 (35) ^f	20.5 (21)	28.8 (67 ^g)
6	13.0 (2714)	+18.6	5.2 (86)	16.2 (43) ^f	21.6 (35)	n.o.
7	8.2 (2729)	+18.2	143.5 (54)	13.7 (34) ^f	18.9 (24)	26.6
8,8'	23.4 (2964)	+40.1	-1.6		19.4	31.6
	23.0 (2959)	+39.7				
9	10.2	+26.3	3.4	19.5	21.5	32.1 (20 ^g)
10	-16.1	+0.6	4.7	14.6	20.4	24.4 (19 ^g)
11	-11.0	+5.7	6.8	17.7	19.9	30.6 (19 ^g)
12	-22.5 (126 ^g)	-5.8	5.4	14.9	20.7	28.0
13	-14.3 (247 ^g)	+1.2	5.0	18.0	20.4	32.6
14	-8.9	+7.8	8.8	19.6	21.9	30.5 (20 ^g)
14'	-5.5	+11.2	7.5	20.8	22.4	31.5 (20 ^g)

^a Measured at 100.6 (¹³C) or 162.1 MHz (³¹P), Bruker WM400 spectrometer, CDCl₃ solution. ^b ¹J_{PtP} (hertz) in parentheses. ^c Coordination shift: see text. ^d R = Me or Ph as appropriate. ^e ²J_{PtC} in parentheses. ^f ²J_{PtC} in parentheses. ^g Triplets due to virtual coupling, see text. ^h ²J_{PC}. ⁱ ¹J_{PC}. ^j ²J_{SnP}.

(>72 h) when the starting materials were heated together in refluxing THF.

ii. RuH[SiMe(CH₂CH₂CH₂PPh₂)₂](CO)₂ (18**).** A sealed-tube reaction between MeSiH(CH₂CH₂CH₂PPh₂)₂ (0.24 g, 0.48 mmol) and Ru₃(CO)₁₂ (0.11 g, 0.17 mmol) conducted as described in **C.i** led to slow deposition, on cooling, of a small amount of a yellow product as fine microcrystals (*ca.* 8% yield), which after redissolution in a minimum of diethyl ether slowly formed as larger crystals that were suitable for X-ray diffraction. Anal. Calcd for C₃₃H₃₆O₂P₂RuSi: C, 60.40; H, 5.53. Found: C, 60.21; H, 5.30.

X-ray Crystal Structure Determinations: Complexes 5, 9, 13, and 18. The general methodology has been described earlier,¹ and similar crystallographic procedures were followed in the present work. Unit cell parameters were obtained by least squares on the setting angles for 25 reflections in each case with 2θ > 30°. The structures were solved by direct methods. Refinement was by least squares. Non-hydrogen atoms were refined anisotropically, except in the case of **18** where the phenyl carbons were refined isotropically. Full details are provided in the Supporting Information, together with the tables of data.

Results

A. Platinum(II) Chemistry. Addition of MeSiH(CH₂CH₂PPh₂)₂ (biPSiH) to Pt(COD)Cl₂ (COD = cycloocta-1,5-diene) in the presence of NEt₃ led to isolation of a white product in essentially quantitative yield that, similar to²³ platinum group metal complexes of perphenylpolyphosphines including PPh₂(CH₂)_nPPh₂ (dppm, *n* = 1; dppe, *n* = 2) or PPh[(CH₂)_nPPh₂]₂ (tpe, *n* = 2; ttp, *n* = 3), was very insoluble in solvents suitable for NMR spectroscopy. On the basis of the microanalytical data, as well as by analogy with the way¹⁰ in which the simple chel precursor Ph₂PCH₂CH₂SiHMe₂ attaches at Pt, this product was formulated as a Pt(II) species Pt[(PPh₂CH₂CH₂)₂SiMe]Cl, **1**, with a putative structure in which the bis(phosphinoalkyl)silyl ligand occupies three sites at the square metal center. A family of related complexes **2–7** that possessed much better solubility properties was obtained by introduction of Cy (cyclohexyl) in place of Ph at P or by increasing the number of backbone methylenes from two to three; one of these (**4**) contains an unsymmetrical ligand framework in which the meth-

ylene chains (*n* = 2) terminate at nonidentical phosphorus donor sites (*i.e.*, PCy₂ vs PPh₂); while a further compound (**5**) was obtained as crystals suitable for X-ray structure determination. Details of the latter, which are discussed below, verify that the biPSi ligand does indeed fit around the Pt center as a tridentate unit, with the chloride ligand completing the coordination of d⁸ Pt(II) with the anticipated square geometry. The two faces of the latter are nonidentical, however: the Me group attached to Si projects in one direction, while the buckling of the C₃ methylene backbones intrudes into the other. Such an arrangement possesses idealized C_s symmetry, in which a single plane σ lies perpendicular to the direction of the metal–ligand bonds (not across the latter, like σ_h of regular d⁸ systems in the D_{4h} point group), relating the –PR₂ groups of the biPSi skeleton. NMR data for compounds **2–7**, which are collected in Table 1, are all in precise accord with this structural model.

Reactions of the biPSiH ligand precursors with Pt(COD)Cl₂, Pt(COD)Me₂, or Pt(COD)(Me)Cl in the absence of NEt₃ or using NaHCO₃ as a base yielded mixtures of products (³¹P NMR). Compounds containing the –PCy₂ group were observed to be more reactive than Ph analogues, with NMR samples showing obvious signs of deterioration after several hours. Mass spectra obtained by using FAB contained prominent fragment ions corresponding to loss of Cl from a molecular ion corresponding to each proposed structure. Treatment of the crystallographically characterized prototype **5** with HCl (*ca.* 1 mol equiv, standardized in benzene solution) afforded a material that was shown by ³¹P NMR spectroscopy to be a mixture (δ 23.4 (¹J_{Pt,P} = 2964 Hz), 23.0 (¹J_{Pt,P} 2959 Hz)), attributable to Pt–Si bond-cleavage centered on either of the distinguishable faces of the molecule (see **B**), to yield a pair of diastereomers **8,8'** (*ca.* 1:4 ratio). Using acetyl chloride in methanol as a source of HCl to try to control the stoichiometry more accurately, a *ca.* 9:1 diastereoisomer distribution was obtained, the major constituent of which was clearly a platinum(II) *trans*-hydrochloride, with ν_{Pt–H} (IR) at 2220 cm⁻¹, ¹J_{PtH} = 1263 Hz (in a triplet resonance at -16.2 ppm, ²J_{PH} = 12.2 Hz, ¹H NMR, see Table 1), *i.e.*, wavenumber, coupling constant, and chemical shift all typical for Pt–H *trans* to the weakly *trans*-influencing chloride ligand.

(23) (a) Chatt, J.; Eaborn, C.; Ibekwe, S. D.; Kapoor, P. N. *J. Chem. Soc. A* **1970**, 1343. (b) Letts, J. B.; Mazanec, T. J.; Meek, D. W. *Organometallics* **1983**, *2*, 696.

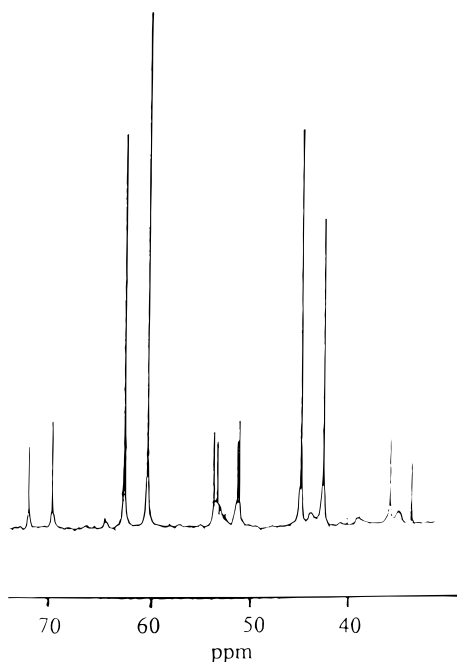


Figure 1. The ^{31}P NMR spectrum (101.3 MHz) of $\text{Pt}[(\text{PCy}_2\text{-CH}_2\text{CH}_2)\text{Si}(\text{CH}_2\text{CH}_2\text{PPh}_2)\text{Ph}]\text{Cl}$, **4**, showing signals due to $-\text{PCy}_2$ centered at δ 62.5 ppm and $-\text{PPh}_2$ at 44.9 ppm.

The ^{31}P resonances of the platinum complexes **2–8** were observed as *ca.* 1:4:1 triplet structures, through coupling to ^{195}Pt , with the magnitude of $^1J_{\text{PtP}}$ in the range 2714–2981 Hz, indicative of a *trans* disposition for the two equivalent phosphorus atoms. The chemical shift difference $\Delta\delta$ ^{31}P between an uncomplexed phosphinoalkylsilane and its phosphinoalkylsilyl complex²⁴ is also informative, being rather large (54–61 ppm deshielded on complexation) for coordination through formation of five-membered chelate rings but more modest ($M = \text{Pt}$) for P in six-membered cyclic framework geometries. The ^{31}P NMR spectrum of the single product **4** in which the substituents on the two P atoms are different is observed as an *abx* array, as depicted in Figure 1. The latter highlights (a) the chemical shift difference between δ $-\text{PPh}_2$ and $-\text{PCy}_2$ (the assignment of which parallels that for the silane precursors, *i.e.*, $\Delta\delta$ *ca.* 55 ppm in each case, Table 1), with the former more shielded by almost 20 ppm; (b) the effect of coupling to ^{195}Pt (*i.e.*, *x* in *abx*); (c) most significantly, the magnitude of $^2J_{\text{PP}}$ which at 367 Hz is typical²⁵ for mutually *trans* P atoms. The 10-membered chelate arrangement assigned to the diastereomers **8**, **8'** results in $\Delta\delta$ *ca.* 40 ppm.

B. Iridium(III) Chemistry. Preliminary investigation of the corresponding iridium chemistry using the phosphinoethylsilyl precursor again afforded products with very limited solubility; but the bis(phosphinopropyl)silane, biPSiH (*i.e.*, C_3 backbone), reacted immediately with $[\text{Ir}(\text{COD})\text{Cl}]_2$, with the yellow color of the latter darkening to afford an orange reaction mixture, from which a soluble, deep orange complex (**9**) was isolated in excellent yield. This was formulated on the basis of microanalytical data and multinuclear NMR spectroscopy as a five-coordinate analogue $\text{IrH}[\text{SiMe}(\text{CH}_2\text{CH}_2\text{CH}_2\text{PPh}_2)_2]\text{Cl}$ of the distorted trigonal-bipyra-

Table 2. IR and ^1H NMR Data for Iridium(III) Complexes

compd	$\nu(\text{M-H})/\text{cm}^{-1}$	$\nu(\text{CO})/\text{cm}^{-1}$	δ M-H/ppm ($^2J_{\text{PH}}/\text{Hz}$)
9	2200		-22.38 (14.7)
10	2244	2030	-18.16 (11.7)
11	2120	1979	-6.09 (15.7)
12	n.o.	2046	-11.87 ^a (11.5)
13	2123	1990	-8.43 ^b (13.2)
14	2044,2022 ^c	1942 ^{c,d}	-8.61 ^e (16.4), -9.98 ^{f,g} (16.8)
14'	(2044,2022 ^c)	(1942 ^c)	-8.84 ^e (16.4), -10.93 ^{f,h} (19.0)
15	n.o.	n.o.	-9.51 (16.3), -9.69 (14.1)
16	n.o.	n.o.	-10.50 (15.9) ⁱ

^a $^2J_{\text{SnH}} = 1072$ Hz. ^b $^2J_{\text{SnH}} = 172$ Hz. ^c IR for **14/14'** mixture. ^d $\nu(\text{CO})$ at 1952 cm^{-1} *trans* to H, 2001 *trans* to ^2H in ^2H isotopomer mixture **14a/14'a**. ^e H *trans* to Si. ^f H *trans* to CO. ^g $^2J_{\text{HH}} = 5.1$ Hz. ^h $^2J_{\text{HH}} = 4.4$ Hz. ⁱ $^2J_{\text{PH trans}} = 104$ Hz.

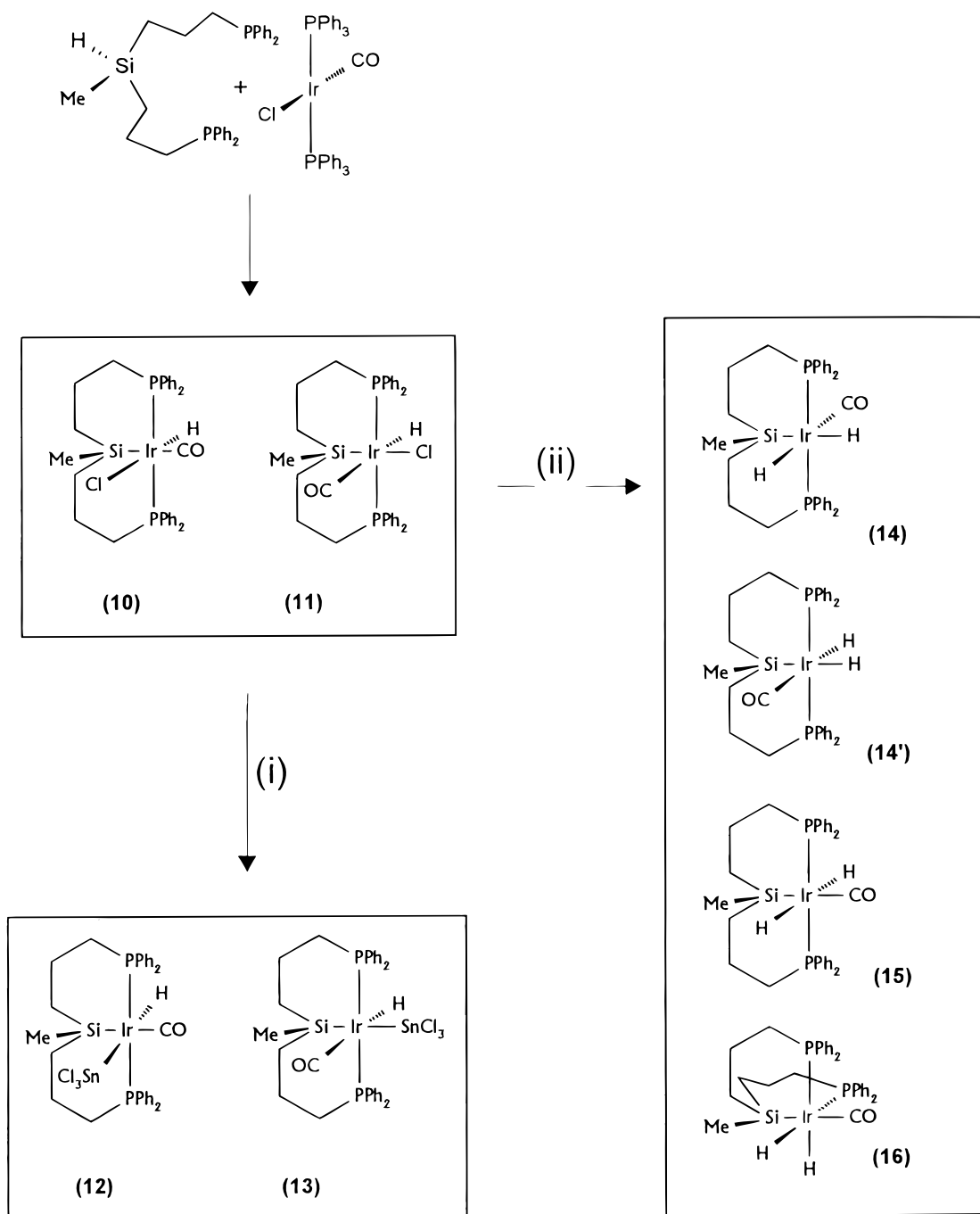
midal (dist-TBP)²¹ chel complex¹ $\text{Ir}(\text{SiMe}_2\text{CH}_2\text{CH}_2\text{PPh}_2)_2\text{-Cl}$, analogy with the latter suggesting^{1,21} an axial-equatorial-axial relationship for the P,Si,P ligating atoms of the biPSi framework. Thus, a single high-field resonance at δ -22.38 in the ^1H NMR is split into a triplet by coupling to two equivalent P atoms of the biPSi ligand, with $^2J_{\text{PH}} = 15$ Hz establishing a *cis* relationship of H with P. A broad, weak absorbance in the IR at *ca.* 2200 cm^{-1} is attributable to $\nu_{\text{Ir-H}}$. The molecular structure of $\text{IrH}(\text{biPSi})\text{Cl}$ (**9**) has been established definitively by X-ray structure determination (see below), which in addition to confirming the proposed disposition of the biPSi unit identifies an *anti* relationship across the metal center of H (at Ir) *vs* Me (at Si).

Reaction between *trans*- $\text{Ir}(\text{PPh}_3)_2(\text{CO})\text{Cl}$ (Vaska's Complex) and biPSiH afforded a product formulated on the basis of NMR spectroscopy as a 3:1 mixture of two octahedral stereoisomers **10** and **11** (see Scheme 1) of the Ir(III) complex $\text{IrH}(\text{biPSi})(\text{CO})\text{Cl}$. The high-field region of the ^1H NMR spectrum contained two triplets, with that due to the major product (**10**, with δ ^{31}P -16 ppm) at δ -17.2 with $^2J = 11.7$ Hz, *i.e.*, characteristic^{9a,10,11} of H *trans* to Cl; while the resonance due to the less abundant isomer (**11**, δ ^{31}P -11 ppm) is centered at -6.09 ppm ($^2J_{\text{cis}} = 15.7$ Hz), consistent with H *trans* to a strongly *trans*-influencing ligand, *i.e.*, CO. Fractional crystallization afforded the major isomer (**10**) as an analytically pure methylene chloride monosolvate, the IR spectrum of which showed (in addition to bands similar to those of the ligand precursor) a weak absorption at 2244 cm^{-1} assigned to $\nu_{\text{Ir-H}}$, together with a much stronger peak at 2030 cm^{-1} attributable to ν_{CO} . Using these assignments, it was possible to also identify the corresponding vibrations in isomer **11** at 2120 and 1979 cm^{-1} .

Reaction of the **10:11** mixture with tin(II) chloride in THF solution afforded (NMR) an iridium-tin complex $\text{IrH}(\text{biPSi})(\text{CO})\text{SnCl}_3$ as another pair of stereoisomers (**12** and **13**) in the same 3:1 ratio. This time the minor isomer (**13**) crystallized preferentially ($\text{CH}_2\text{Cl}_2/\text{Et}_2\text{O}$), giving material suitable for X-ray diffraction. The molecular structure, which is discussed further below, confirms an octahedral iridium(III) geometry in which H and CO are *trans* to one another, and a distorted trichlorostannyl ligand occupies a site *trans* to the Si of the tridentate *mer*-biPSi framework (Scheme 1). In the IR, compound **13** showed bands at 2123 and 1990 cm^{-1} (Table 2) attributed to $\nu_{\text{Ir-H}}$ and ν_{CO} , respectively, with the latter at 2046 cm^{-1} in **12** (*trans* to Si). The high-field ^1H NMR spectrum was again informative: com-

(24) Garrou, P. E. *Chem. Rev.* **1981**, *81*, 229.

(25) Al-Salem, N. A.; Empsall, H. D.; Markham, R.; Shaw, B. L.; Weeks, B. J. *Chem. Soc., Dalton Trans.* **1979**, 1972.

Scheme 1^a

^a Reagents: (i) SnCl₂/THF; (ii) LiAlH₄/THF.

pound **13** gave rise to a triplet, $\delta -8.43$ with *cis* coupling to ³¹P and ^{117,119}Sn (13.2, 172 Hz, Table 2), while the corresponding resonance for isomer **12**, centered at $\delta -11.87$, showed a much bigger ²J_{Sn,H} of 1072 Hz (*trans*) with ²J_{P,H} = 11.5 Hz. Singlet SiCH₃ signals (δ 0.08 and -0.21 ppm for **12** and **13**, respectively) showed coupling to tin (⁴J = 28.1 Hz) only for **13**, in which Si is *trans* to Sn.

Treatment of the stereoisomer mixture **10:11** with LiAlH₄ in THF afforded a product shown by NMR to be a mixture of isomers of the dihydride IrH₂(biPSi)(CO). The high-field portion of the ¹H NMR spectrum is illustrated in Figure 2. Two pairs of signals in *ca.* 3:1 ratio (Table 2) appear as triplets (each *J* = 16.4 Hz) of doublets (*J* = 4.4, 5.1 Hz) attributable to two *mer*-biPSi diastereomers **14** and **14'**, Scheme 1, in which the H

couples to two equivalent *cis* P atoms as well as geminally to a single *cis* H. Thus, either diastereomer shows two resonances, of which, on the basis of relative *trans* influences that to lower field may tentatively be assigned to H *trans* to Si with the upfield resonance due to H *trans* to CO (Table 2). The spectra of two additional minor constituents are superimposed (Figure 2). The first, which is evident as a pair of triplets near $\delta -9.5$ (Table 2), is assigned to the *trans* dihydrido isomer **15** of **14,14'**, with ²J_{PH} = 16.3, 14.1 Hz and no resolvable coupling between *trans* H atoms. Selective deuteration experiments supported this interpretation: thus, in the ¹H NMR, the ²H isotopomers **14a,14'a** of **14,14'**, produced by reaction of **10** and **11** with LiAl²H₄, presented triplet resonances like those of Figure 2 in which, however, the doublet splittings

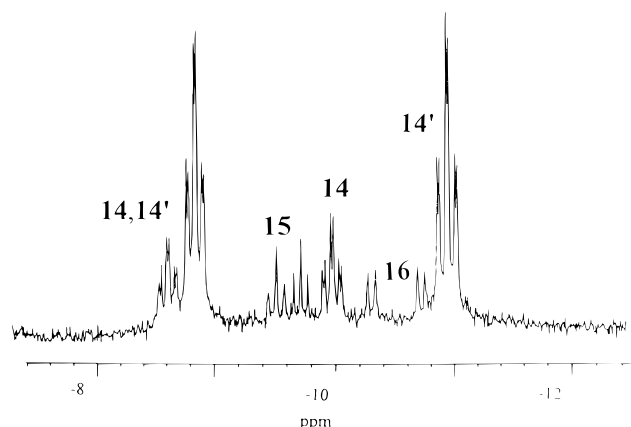


Figure 2. High-field ^1H NMR spectrum (250 MHz) of a mixture of dihydrido-iridium(III) complexes $\text{IrH}_2(\text{biPSi})(\text{CO})$, mainly the diastereomers **14, 14'** (1:3 ratio) together with stereoisomers **15** and **16**. Assignment of the signals specifically to **14** vs **14'** is ambiguous and could be reversed, and likewise distinction between H_{syn} and H_{anti} (vs Me at Si) of **15** is not attempted (see text and Scheme 1).

($^2J_{\text{HH}_{\text{cis}}}$) were absent while that of compound **15a**, *i.e.*, *trans*- $\text{IrH}^2\text{H}(\text{biPSi})(\text{CO})$, was unchanged from that of **15**. Finally an *ab*-like pattern centered at -10.5 ppm is attributed to a *fac* isomer **16**, with the two equivalent H atoms coupling to *trans* P ($^2J = 104$ Hz) as well as *cis* P ($^2J = 15.9$ Hz). This latter conclusion is supported by the observation (^1H NMR) that the same compound (**16**) is formed, initially as the sole hydrido product, when the five-coordinate complex **9** is allowed to react with LiAlH_4 under an atmosphere of CO, although progressive isomerization to **14, 14'** is detectable over 24 h (see Scheme 1).

C. Ruthenium(II) Chemistry. Simple PSi chelate precursors including chelH react with $\text{Ru}_3(\text{CO})_{12}$ at elevated temperature under sealed-tube conditions to afford only moderate yields (*ca.* 35%) of mononuclear Ru(II) homologues $\text{Ru}(\text{chel})_2(\text{CO})_2$: these complexes adopt a *trans* dicarbonyl geometry with chel Si atoms *cis* to one another.¹⁷ We have found that although similar reactions with the biPSi precursors $\text{MeSiH}[(\text{CH}_2)_n\text{PPh}_2]_2$ ($n = 2$ or 3) yield mainly intractable material, adventitious recovery is possible, although in very poor yield, of yellow products that are identifiable as hydrido(dicarbonyl)Ru(II) analogues $\text{RuH}\{\text{SiMe}[(\text{CH}_2)_n\text{PPh}_2]_2\}(\text{CO})_2$ (**17**, $n = 2$; **18**, $n = 3$) on the basis of microanalytical data. Each of these compounds showed a high-field triplet resonance in the ^1H NMR (**17**, $\delta -8.97$, $^2J_{\text{PH}} = 17$ Hz; **18**, $\delta -6.29$, $^2J_{\text{PH}} = 18$ Hz) due to *cis* coupling of a Ru-H to the two P atoms of the tridentate PSi ligand, with a chemical shift suggesting H *trans* to CO. The more soluble of the pair (**18**) crystallized out of solution and was structurally characterized by using X-ray diffraction (see below): the molecule possesses octahedral geometry about Ru(II) in which two carbonyl groups are *cis* and the tridentate biPSi framework is *mer*; the H at Ru (not located) clearly occupies the sixth site, that adjacent to Me (at Si), *i.e.*, a *syn* disposition that is the opposite of the *anti* configuration adopted in the hydrido-iridium complex (**9**).

Conformational Properties of the Bicyclic biPSi Framework. In the ^1H NMR spectra of complexes **2–4** and **6**, in which the biPSi framework terminates in $-\text{PCy}_2$ groups, all methylene hydrogen signals (8 or 12

H, backbone; 48 H, Cy) are compressed into an unresolved envelope in the δ 0.9–2.5 ppm range; while with Ph substituents (at P or Si, *i.e.*, in compounds **3–5** and **7**), there are additional resonances to low field, as expected. For the structurally characterized compound **5**, the backbone hydrogens of the biPSi framework appear as broad signals at δ 0.89 (4 H, on C_α , adjacent to Si) and 2.00 (4 H, on C_γ , adjacent to P) but the central C_βH_2 pair are widely split at δ 1.71 (2 H) and 2.30 (2 H) ppm. This is accompanied by a shift away from the main Ph contour (δ 6.9–7.1, 12 H) of ortho Ph hydrogens to δ 7.6 and 8.1 ppm (4 H each, d, $^3J = 5.5$ Hz); we attribute this substantial deshielding effect to steric interaction with axial β -methylene hydrogens, so also dispersing the latter. In agreement with this interpretation, in the X-ray crystal structure of complex **5**, the carbons atoms that are ortho on axial Ph and β in the backbone approach one another to within 3.35 Å.

The ^1H NMR spectrum of pure **10** showed SiCH_3 at $\delta -0.09$ ppm, with a set of six methylene signals to low field that (at 400 MHz) were unusually well-resolved (by comparison with those for **9** or the platinum biPSi complexes), centered at δ 0.6 (apparent dd, $J = 13.7$ and 3.4 Hz) and 1.09 (apparent td, $J = 13.8$ and 3.5 Hz) due to $\text{C}_\alpha\text{H}_2$ (*i.e.*, α to Si), 1.65 and 2.34 (both br) due to C_βH_2 , and 2.50 (d, $J = 12.9$ Hz) and 3.25 (apparent t, $J = 12.4$ Hz), due to $\text{C}_\gamma\text{H}_2$. Homonuclear decoupling with irradiation into the resonance at δ 2.34 collapsed the smaller coupling in both $\text{C}_\alpha\text{H}_2$ multiplets; while irradiation at the frequency corresponding to δ 1.65 collapsed the triplet structures in δ 1.09 and 3.25 to doublets, $J = 13.0$ and 13.7 Hz, respectively. Relating these observations to the solid state structures of compounds **5** and **9**, in which the biPSi framework adopts a distorted double half-chair conformation (X-ray, see below), a partial analysis is suggested that puts the resonances at δ 1.09, 1.65, and 3.25 due to axial hydrogens, *i.e.*, with $J_{\text{ax-eq}} = 3.5$ Hz, $J_{\text{ax-ax}} = 13$ Hz, and $J_{\text{gem}} = \text{ca. } 12$ Hz, and is in agreement with the assignment for the axial C_βH_2 pair in **5**. The ^1H NMR spectrum of isomer **11** was similar to that of **10**, although less well-resolved. Methylene hydrogens for purified **13** also appeared as six envelopes (δ 0.86 (dd), 1.00 (td), 1.91 (br), 2.39 (br), 2.42 (t), 3.15 (d)), *i.e.*, very similar to the pattern observed for complex **10**.

The appearance of the ^{13}C NMR spectra is governed by two important general criteria. Firstly, while the idealized geometries for all of the complexes possess only planar symmetry (point group C_s), the single plane does relate backbone methylene carbon atoms that are α , β , and γ to Si and also carbon atoms of pairs of substituents R in the phosphino fragments $-\text{PR}_2$ (although not pairs of atoms within each R). Secondly, the magnitude of $^2J_{\text{PP}}$ (*ca.* 350 Hz, *q.v.*) is sufficiently large compared with $^1J_{\text{PC}}$ (12–17 Hz in the silane precursors, simulated at 38 Hz for compound **5**) that resonances due to carbon atoms α to P are observed as *triplets*, through²⁶ virtual coupling (Table 1). Coupling of backbone carbons to ^{195}Pt is also observed for compounds **2–7**. The low-

(26) Becker, E. D. *High Resolution NMR*; Academic Press: New York, 1969.

(27) Brinkley, C. G.; Dewan, J. C.; Wrighton, M. S. *Inorg. Chim. Acta* **1986**, *121*, 119.

(28) Heyn, R. H.; Huffman, J. C.; Caulton, K. G. *New J. Chem.* **1993**, *17*, 797.

(29) Campion, B. K.; Heyn, R. H.; Tilley, T. D. *J. Chem. Soc., Chem. Commun.* **1992**, 1201.

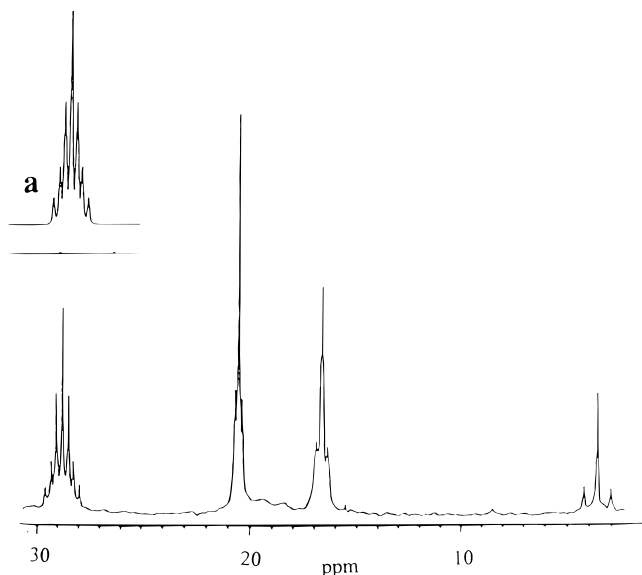


Figure 3. The ^{13}C NMR spectrum (62.9 MHz) of Pt(biPSi)-Cl, **5**, showing signals progressively to high frequency due to C_{Me} , C_{α} , C_{β} , and C_{γ} , with the inset being a spectral simulation of the fine structure of the C_{γ} resonance (see text).

frequency (*i.e.*, high-field) region for compound **5** illustrates this effect (Figure 3). Four signals that are progressively less shielded are assigned to C_{Me} , C_{α} , C_{β} , and C_{γ} , respectively (*i.e.*, α , β , γ to Si; C_{γ} adjacent to P), exhibiting coupling to platinum of 75 (2J), 35 (2J), 21 (3J), and 67 Hz, the latter confirmed by spectral simulation (*abmx* spin system, Figure 3). Only partially resolved triplet structure in the Me and C_{α} resonances is attributable to very small 3J , to the two P atoms *cis* to Si; but C_{γ} is split by virtual triplet structure, with much bigger $|^1J_{\text{PP}} + ^3J_{\text{PC}}| = 38$ Hz (simulated with $^1J = 38$ Hz, $^3J = 0$ Hz, Figure 3). Resonances at 133.7 and 135.1 ppm, which are assigned to the inequivalent ortho C atoms in each Ph group at P, also appeared as triplets, J (*i.e.*, $|^2J + ^4J|$) = 6 Hz; the same situation was evident for inequivalent C_{α} of cyclohexyl substituents at P, where these could be distinguished from other methylene resonances (*e.g.*, in complex **2**, δ 33.4 and 35.1 are apparent triplets with $J = 14$ Hz); a similar pattern for C_{γ} and C_{ortho} was repeated as a characteristic of the family of complexes (Table 1).

Compound **7**, in which Ph is attached at Si as well as at P, gave rise to a collection of ^{13}C signals in the 125–135 ppm range that could be assigned similarly on the basis of triplet splitting with *ca.* 1:4:1 multiplicity (coupling to ^{185}Pt) vs a 1:2:1 array (virtual coupling to ^{31}P). Thus, for Ph on Si, δ C^1 143.5 ppm ($^2J = 54$ Hz), C^2 135.3 ($^3J = 27$ Hz), C^3 , C^4 (singlets, $J = 126.8, 127.5$); while for the two symmetry unrelated Ph groups on P, δ C^1 131.0, 133.2 ($J = 27, 28$ Hz), C^2 133.2, 135.5 ($J = 5, 6$ Hz), C^3 127.9, 128.0 ($J = 5, 5$ Hz), and C^4 129.9, 130.1. Assignments for the methylene carbons in the chemically distinct backbones of complex **4** (*i.e.*, α or β to Si) are ambiguous (see Table 1), and in the diastereomers **8**, **8'** those α and β to Si overlap with one another around δ 18.4 ppm.

X-Ray Crystal and Molecular Structures of Complexes 5, 9, 13, and 18. Crystal data for the four-coordinate platinum(II) (**5**), five-coordinate iridium(III) (**9**), and six-coordinate iridium(III) (**13**) and ruthenium-

(II) (**18**) complexes are collected together in Table 3. The molecular geometries are illustrated in Figures 4–7 respectively, where important bond distances and angles are listed in the caption in each case; the spatial arrangement adopted by the tridentate biPSi framework introduces a regularity amongst the four structures that is immediately striking. Positional parameters are included in the Supporting Information, which also contains full tables of bond distances and angles.

Angles between the four ligating atoms at the metal center in **5** are all very close to 90° , consistent with square coordination as expected for d^8 Pt(II). The two faces so formed are clearly distinguished; however, the methyl group at Si projects tetrahedrally into one, while the other accommodates the backbones that connects Si with P (Figure 4). The skeletal geometry of the biPSi unit completes two six-membered ring systems that are fused along the Pt–Si bond, with the polymethylene bridges twisted into a double half-chair conformation that allows the Me at Si and one Ph at each P to be identified as axial groups. Such a stereochemistry supports the interpretation of the NMR data, although in the crystal the two biPSi phosphinopropyl groups are not symmetry related, *i.e.*, the idealized σ (C_s point group) is not a crystallographic plane. The P–Pt–P and Si–Pt–Cl angles are each distorted away from linearity (176° , 173° , respectively), both in the same sense, *i.e.*, toward the methyl at Si. At 2.285 (mean) and 2.307 Å, the Pt–P and Pt–Si bond distances lie within the narrow ranges that are typical for related structures; the Pt–Cl bond length at 2.436(6) Å (*trans* to Si) is measurably longer than corresponding distances¹² *trans* to either H or Me, Table 4.

The molecular structure of the five-coordinate complex **9** closely resembles that of the platinum compound **5** in terms of the disposition of the biPSi skeleton (Figure 5). More significantly, it bears an obvious relationship to the geometry of its analogue¹ Ir(chel)₂-Cl (chel = $-\text{SiMe}_2\text{CH}_2\text{CH}_2\text{PPh}_2$), which with the P atoms axial and the two equatorial Si centers separated by an angle less than 90° typifies the dist-TBP configuration recognized recently by Eisenstein *et al.*^{21a} For Ir(chel)₂Cl, this leads to wide equatorial angles of $134.8(2)^\circ$ and $138.9(2)^\circ$ to the weak Cl member of the five-coordinate ligand set. For **9**, the corresponding Si–Ir–Cl angle is less obtuse, $127.2(1)^\circ$, with the chloride and the methyl group on Si being *syn*, *i.e.*, occupying the same molecular face (defined by the ax–eq–ax biPSi unit). This implies that the hydride ligand is bonded to Ir on the opposite face, *i.e.*, it is *anti* vs Me at Si, thereby resolving a structural ambiguity presented by the spectroscopic data, which offer no distinction between the *syn* vs *anti* diastereomers of **9**. It may be inferred that if the position of the hydrogen atom subtends a characteristically narrow angle Si–Ir–H (possibly $< 90^\circ$), *i.e.*, with H–Ir–Cl *ca.* 140° like¹ Si–Ir–Cl in Ir(chel)₂Cl, it will occupy a pocket generated by the puckering of the biPSi polymethylene skeleton. The structural relationship of **9** with Ir(chel)₂Cl (which is¹ dist-TBP²¹) is further reinforced by Ir–P and Ir–Si bond lengths that are almost equal (near 2.3 Å), with the equatorial bond Ir–Cl conspicuously short¹ at 2.399(2) Å, Table 4.

The arrangement of the tridentate biPSi ligand around distorted octahedral d^6 Ru(II) in compound **18**

Table 3. Crystal Data^a for Compounds 5, 9, 13, and 18

	5	9	13	18
chem formula	PtP ₂ SiClC ₃₁ H ₃₅	IrP ₂ SiClC ₃₁ H ₃₆	IrSnCl ₃ P ₂ SiOC ₃₂ H ₃₆	RuP ₂ SiO ₂ C ₃₃ H ₃₅
fw	728.2	726.3	944	654.8
cryst syst	monoclinic	monoclinic	orthorhombic	orthorhombic
space group	<i>P2</i> ₁ / <i>a</i>	<i>P2</i> ₁ / <i>n</i>	<i>Pna</i> 2 ₁ (No. 33)	<i>P2</i> ₁ 2 ₁ 2 ₁
<i>Z</i>	8	4	4	4
<i>a</i> , Å	21.581(2)	11.039(1)	26.073(3)	8.895(2)
<i>b</i> , Å	12.714(2)	24.322(1)	18.048(3)	9.858(1)
<i>c</i> , Å	22.119(2)	11.318(1)	8.761(2)	36.048(3)
<i>B</i> , deg	94.50(3)	97.79(4)	90	90
<i>V</i> , Å ³	6050(3)	3010(2)	4122.6	3160.9
<i>F</i> (000)	2848	1440	1831.81	1349
<i>Q</i> calcd, g cm ⁻³	1.58	1.6	1.521	1.38
μ (Mo K α), cm ⁻¹	48.51	44.91	45.38	5.85
no. of rflns colld	3421	6461	2909	1737
no. of unique rflns	2735	3268	2074	1607
no. of rflns obsd (<i>I</i> > 3 σ (<i>I</i>))				
no. of variables	325	325	349	227
<i>R</i> ^b	0.0876	0.0375	0.0779	0.0619
<i>R</i> _w ^b	0.0841	0.0449	0.0762	

^a All data were collected with graphite-monochromated Mo K α radiation ($\lambda = 0.0709\ 26\ \text{\AA}$) at 291 K using a CAD4 diffractometer. Scan type, $\omega-2\theta$; scan range θ , $(1.35 + 0.35\text{scan}\theta)^\circ$; $2\theta_{\text{max}}$, 46.0° throughout. ^b $R = \sum(|F_o| - |F_c|)/\sum|F_o|$; $R_w = \sum w|F_o| - |F_c|)^2/\sum w|F_o|^2$.

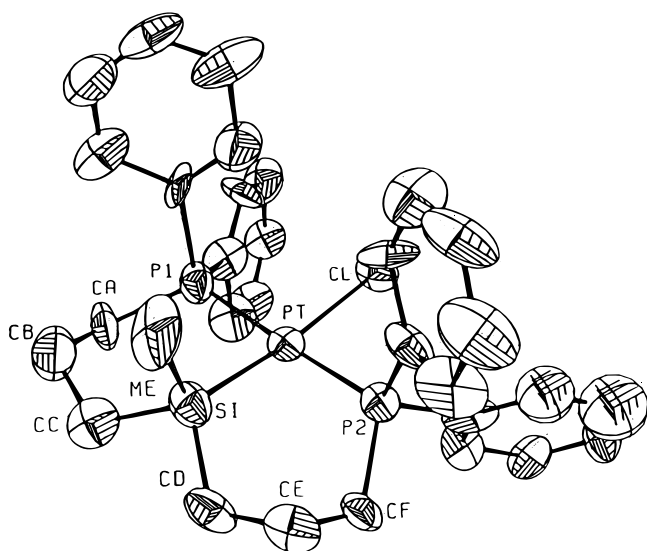


Figure 4. Molecular geometry of complex **5**. Selected bond lengths (Å) and angles (deg): Si–Pt, 2.307(8); P(1)–Pt, 2.289(9); P(2)–Pt, 2.280; Si–Pt–Cl, 172.8(3); P(1)–Pt–Cl, 89.5(3); P(1)–Pt–Si, 89.9(3); P(2)–Pt–Cl, 90.6(3); P(2)–Pt–Si, 89.4(3); P(2)–Pt–P(1), 175.7(3).

is again the focus of the structure, setting up a *mer* geometry (Figure 6) that mirrors the in-plane character of PSiP ligation in **5** or **9**. The hydride ligand was not located, but its position is indicated by a vacant position that is (unlike that in **9**) adjacent to the Me group on the Si atom. Coordination at the metal is completed by a *cis* dicarbonyl unit, in which C–Ru–C is opened up to $105.8(12)^\circ$, although the Si–Ru and Ru–C(8) bonds are oriented almost exactly perpendicularly. Thus, the C(7)–Ru vector points nearly 20° away from a directly *trans* relationship with the Si–Ru bond, *i.e.*, the carbonyl group *trans* to Si is displaced significantly toward the hydride site. The resulting Si–Ru–C(7) angle at $163.4(10)^\circ$ is, however, equal within error to the Si–Ir–Cl angle (*i.e.*, that also includes a M–H bond) in¹ the isoelectronic complex IrH(chel)(CO)(PPh₃)Cl, where Si is *trans* to Cl rather than CO. The bond distances from Ru to C(7) (*trans* to Si) and C(8) (*trans* to H) are not distinguishable, and Ru–Si at 2.457(7) Å and Ru–P at 2.342 (mean) Å appear to be normal (Table

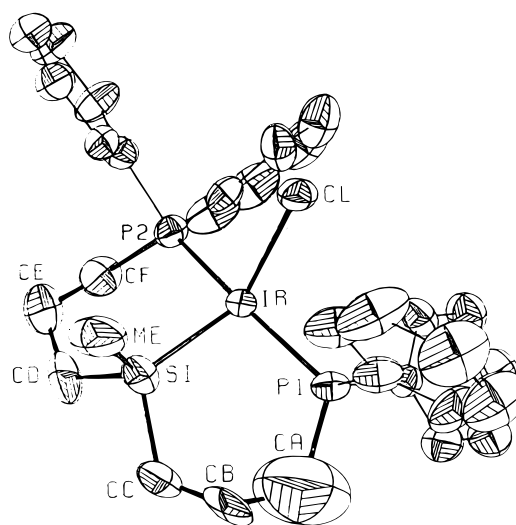


Figure 5. Molecular geometry of complex **9**. Selected bond lengths (Å) and angles (deg): Si–Ir, 2.287(3); Cl–Ir, 2.399(2); P(1)–Ir, 2.302(2); P(2)–Ir, 2.294(2); P(1)–Ir–Cl, 93.3(1); P(2)–Ir–Cl, 91.5(1); P(2)–Ir–P(1), 167.3(1); Si–Ir–Cl, 127.2(1); Si–Ir–P(1), 93.1(1); Si–Ir–P(2), 93.3(1).

4). It is evident that while each of the crystalline products **9** or **18** is a pure constituent of a possible diastereomeric pair (*syn* and *anti*), the observed stereochemistry is the reverse at ruthenium (*syn*-**18**) of that at iridium (*anti*-**9**). This is emphasized in Figure 8, which compares the core geometries for **5**, **9**, and **18**, highlighting that Cl is *syn* vs Me in **9** but CO is *anti* vs Me in **18**, as well as the way in which *syn* vs *anti* approaches (relative to Me on Si) of external substrate to the metal center will differ (*e.g.*, of HCl to Pt, see **B**).

The solid state structure of the six-coordinate iridium(III) trichlorostannyl complex **13** is more irregular than those of **5**, **9**, and **18**: the molecule appears to be sterically crowded and the two cyclic fragments of the biPSi framework are twisted relative to one another along the Ir–Si direction, as shown in Figure 7 (a projection similar to those of Figures 4–6 is included in the Supporting Information). This reduces the P–Si–P angle to $156.2(4)^\circ$ but allows the Me at Si, the carbonyl group on Ir, and the two chlorine atoms of the –SnCl₃ group to stagger with rather than eclipse one

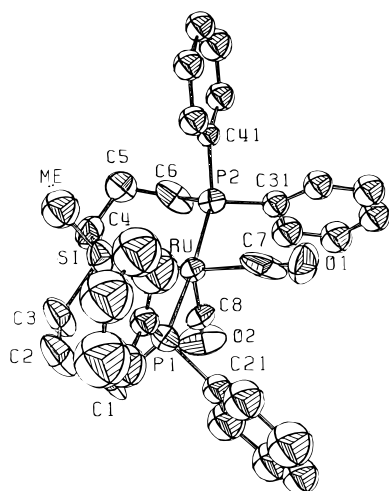


Figure 6. Molecular geometry of complex **18**. Selected bond lengths (Å) and angles (deg): Si–Ru, 2.457(7); P(1)–Ru, 2.348(6); P(2)–Ru, 2.335(6); C(7)–Ru, 1.96(3); C(8)–Ru, 1.98(2); P(2)–Ru–P(1), 174.5(2); Si–Ru–P(1), 87.6(2); Si–Ru–P(2), 88.5(2); C(7)–Ru–P(1), 90.4(7); C(7)–Ru–P(2), 92.2(7); C(7)–Ru–Si, 163.4(10); C(8)–Ru–P(1), 93.8(7); C(8)–Ru–P(2), 90.1(8); C(8)–Ru–Si, 90.9(7); C(8)–Ru–C(7), 105.8(12). The phenyl rings have been simplified for clarity.

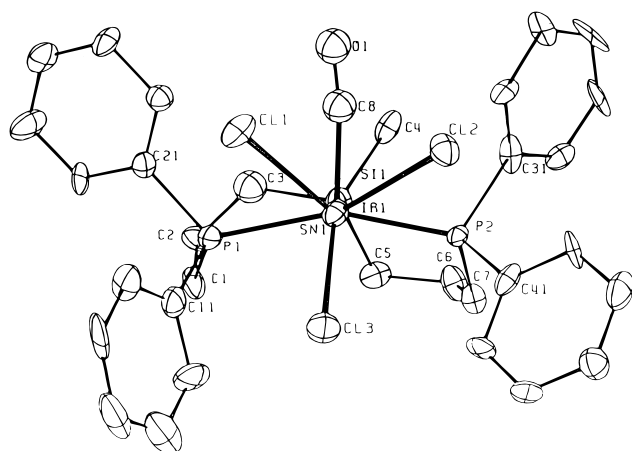


Figure 7. Molecular geometry of complex **13**. Selected bond lengths (Å) and angles (deg): Si(1)–Ir(1), 2.42(2); Sn(1)–Ir(1), 2.658(3); P(1)–Ir(1), 2.37(1); P(2)–Ir(1), 2.31(1); C(8)–Ir(1), 1.93(7); P(1)–Ir(1)–Sn(1), 93.2(3); P(2)–Ir(1)–Sn(1), 94.8(3); P(2)–Ir(1)–P(1), 156.1(4); Si(1)–Ir(1)–Sn(1), 175.8(4); Si(1)–Ir(1)–P(1), 87.9(5); Si(1)–Ir(1)–P(2), 85.8(4); C(8)–Ir(1)–Si(1), 86(2); C(8)–Ir(1)–Sn(1), 90(2); C(8)–Ir(1)–P(1), 102(2); C(8)–Ir(1)–P(2), 100(2).

another along the Si–Ir–Sn vector, which is nearly linear (176°). There is a vacant site *trans* to CO to account for the hydride ligand (not located), putting the latter *anti* vs C(4) (*i.e.*, the Me on Si); its position within the biPSi pocket, especially in relation to C(5), is unknown but could possibly explain why the bond from Ir to P(1) is 0.06 Å longer than that to P(2). The bond distance to Si, 2.42 (2) Å, is normal for octahedral Ir(III) but that to Sn is very long,³⁰ 2.659 (3) Å (Table 4), presumably as a further reflection of the high *trans*-influencing character of the silyl group. The trigonal –SnCl₃ group is distorted from tetrahedral (with Cl–Sn–Cl angles close to 90°), but a similar effect has been observed in related structures.¹⁵

(30) Albinati, A.; Gunten, U.; Pregosin, P. S.; Ruegg, H. J. *J. Organomet. Chem.* **1985**, *295*, 239.

Table 4. M–Ligand Bond Distances (Å) in Silylplatinum, -iridium, and -ruthenium Complexes

compd	M–Si	M–P ^a	M–Cl	ref
Pt(chel) ₂	2.36	2.35 ^b		10a
Pt(biPSi)Cl (5)	2.31	2.29	2.44 ^b	c
<i>trans</i> -PtCl(SiPh ₃)(PPh ₃) ₂	2.32	2.30	2.47 ^b	12
IrH(chel)(CO)(PPh ₃)Cl	2.41	2.31	2.51 ^b	1
Ir(chel) ₂ Cl ^d	2.31	2.30	2.38	1
IrH(biPSi)Cl ^d (9)	2.29	2.30	2.40	c
IrH(biPSi)(CO)SnCl ₃ (13)	2.42	2.31, 2.37	(2.66) ^{b,e}	c
<i>fac</i> -IrH(PMe ₃) ₃ (Me)(SiEt ₃)	2.42	2.30–2.36 ^f		13
RuH(biPSi)(CO) ₂ (18)	2.46	2.34		c
RuH(SiPh ₃)(PPh ₃)(CO) ₃	2.45	2.41 ^b		27
RuH(SiHPh ₂)(P ^t Bu ₂ Me) ₂ (CO) ^g	2.33	2.38		28
RuH ₂ (C ₅ Me ₅)(SiHClmes)P ^t Pr ₃ ^h	2.30	2.35		29

^a Mean, unless otherwise indicated. ^b *Trans* to Si. ^c This work. ^d Five-coordinate cpx, dist-TBP. ^e Ir–Sn distance. ^f See text. ^g Five-coordinate cpx, SQP, apical Si. ^h Ru(IV) cpx.

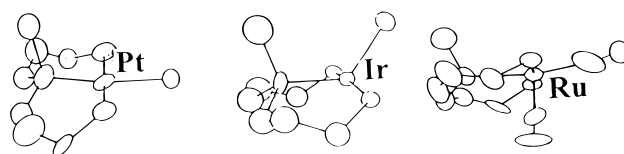


Figure 8. Comparison of the core framework structures in biPSi complexes of Pt (**5**), Ir (**9**), and Ru (**18**). Note the *syn* arrangement of Cl at Ir and Me at Si (both up), but CO at Ru (down) is *anti* vs Me at Si (up), *i.e.*, H at Ir is *anti* (**9**), at Ru is *syn* (**18**) vs Me (at Si).

Discussion

Previously, it has been shown *inter alia* (i) that oxidative addition of Me₂SiH(CH₂)₂PPh₂ (chelH) at Pt(II) or Ir(I) is chelate-assisted and is also regioselective;^{9,10} (ii) that HSi(CH₂CH₂PPh₂)₃ (triPSiH) will displace all three molecules of coordinated triphenylphosphine from RhH(CO)(PPh₃)₃ to afford the novel anchored rhodium(I) silyl Rh(triPSi)(CO);¹⁷ (iii) that complexation of chelH at five-coordinate Ir(I) (which also requires displacement of two PPh₃ molecules) occurs exclusively by coplanar entry of P, Si, and H meridionally to afford the product IrH₂(chel)(CO)(PPh₃) as a single stereoisomer;^{9a,31} (iv) that the latter undergoes slow interchange of hydrogen atoms between the two *cis* octahedral sites.³¹ The coordination behavior of the biPSi framework fits logically into the context established by these observations. Thus, attachment of a bis-(phosphinoalkyl)silyl group (*i.e.*, by chelate-assisted Si–H bond addition, hydrosilylation) leads finally to a wrap-around geometry at square Pt(II) with *trans* P atoms and a Cl ligand retained *trans* to Si (*e.g.*, as in complex **5**). This suggests that H enters at an axial site in a transient, octahedral Pt(IV) configuration PtH(biPSi)Cl₂, a relative of the complex PtH(chel)₂Cl that has been characterized directly^{10b} by NMR, then is lost by *cis* elimination of HCl to afford the observed Pt(II) product.

Unlike most d⁸ complexes (which are planar symmetric, D_{4h}), in the Pt(II) compounds **1–7** reflection will operate perpendicular to the biPSi skeleton (rather than across it) and then only if the conformations of the two chelate rings are identical. The juxtaposition of the methyl group on Si and the backbone methylenes of the biPSi skeleton imposes identical conditions on the

(31) Auburn, M. J.; Stobart, S. R. *J. Chem. Soc., Chem. Commun.* **1984**, 281.

idealized symmetry properties of all the remaining complexes (except **8,8'**), with σ (C_s point group) again perpendicular to the P–Ir–P axis (*i.e.*, bisecting the P–Ir–P angle). The ^1H NMR data indicate that in solution equivalence between the independent polymethylene chains of the bicyclic biPSi unit is established as a result of framework nonrigidity (although in none of the crystal structures are the two sets of nuclei symmetry related). Thus, methylene hydrogens are geminally differentiated, typically giving rise to six distinguishable resonances that (unequivocally for compound **10**) exhibit coupling patterns that are cyclohexane-like. Because the two faces at Pt are nonidentical, detachment of Si from Pt (which takes place with retention of the *trans* phosphine geometry) generates a diastereoisomeric pair (**8,8'**) of hydridoplatinum(II) products (see **B**), with one strongly favored over the other, although which one is not disclosed by the spectroscopic data. The values for $^1J_{\text{PtP}}$ in all the platinum(II) biPSi complexes, at up to 2981 Hz (Table 1), lie at the top end of those reported for systems in which this parameter has been linked³² to the electronic properties of the ligand *cis* to P (*i.e.*, the reverse of the more familiar influence on $^1J_{\text{PtP}}$ of the ligand *trans* to P, where the strongly inductive Si center leads^{10,11,13} to the lowest reported values).

Complex **9**, which is formed by reaction of the silane biPSiH with $[\text{Ir}(\text{COD})\text{Cl}]_2$, crystallizes as a single diastereomer in which H is *anti* vs Me on Si (as shown by X-ray diffraction) and provides another example of a five-coordinate, 16-electron Ir(III) geometry of the type we have structurally characterized¹ previously. Addition of the silane biPSiH to *trans*-Ir(PPh_3)₂(CO)Cl, however, is accompanied by formation of the hydrido-iridium(III) complex IrH(biPSi)(CO)Cl as two stereoisomers, **10** and **11**, that differ in the nature of the ligand *trans* to Si (CO, 75%; Cl, 25%). This is consistent with Si–H bond addition at Ir parallel⁸ to the CO–Ir–Cl axis that follows initial coordination through P. Formation of a large-ring chelate structure (resembling that of diastereomers **8,8'**, **B**), through substitution of PPh_3 by the more basic alkyldiphenylphosphino group of the PSi precursor^{9,10,31} then displacement of the second (*trans*) PPh_3 ligand, will lead to diastereomeric Ir(I) intermediates that can undergo reaction to afford *anti* (**C**) or *syn* (**D**) pairs of products. Observation of two (rather than four) complexes implies that either **10** and **11** have opposite stereochemistry, through stereospecific formation of one *anti* as in **C** and the other *syn* as in **D**, or (more likely) one pair only is formed, exclusively *via* **C** or **D**. Precoordination of biPSiH through a single P atom followed by Si–H bond addition would channel the latter through diastereomeric pathways (resulting from chirality at Si) that would be more likely to result in observation of all four isomers.

Recovery of an identical diastereomer distribution after **10** and **11** are converted to **12** and **13**, together with crystallographic characterization of **13** as *anti*, may suggest that all four are *anti*, as indicated in Scheme 1; thus, while little appears to be known about the specifics of SnCl_2 insertion, any way of forming **13** from a *syn* precursor clearly requires a diastereoisomerization step. The distinction between **12** and **13** is easily made in the ^1H NMR, where $^2J_{\text{SnH}}$ is an order of magnitude

bigger for H *trans* vs *cis* to Sn (Table 2). There is also a more surprising change in $^2J_{\text{SnP}}$ (by a factor of two, Table 1), which is larger with Sn *trans* to Si (**13**) vs *trans* to H (**12**). Treatment of the same stereoisomer distribution **10,11** with hydride (LiAlH_4) directly affords a third mixture of isomers, predominantly **14** and **14'** (1:3 ratio, Figure 2); since each of these is a dihydrido complex with a *mer*-biPSi structure and nonequivalent H atoms (^1H NMR), they are necessarily assigned as *anti* and *syn* diastereomers (see Scheme 1), although the data do not identify which one is the more abundant of the two. Values of *ca.* 5 Hz for $^2J_{\text{HH}(\text{cis})}$ (Table 2) are typical.^{9,20,31,33} The two other minor products of the same reaction are tentatively identified (NMR) as the *trans* dihydrido isomer **15** and the *fac*-biPSi isomer **16** (Scheme 1). If this is correct, complex **15** is a very rare³³ example of a *trans* transition-metal dihydrido complex in which the H atoms are nonequivalent and for which the absence of *trans* H,H coupling is in accord with Karplus-type arguments; values for J_{HH} of 5 and 17.2 Hz, respectively,^{20a,c} have been reported for (formally) Ir(III) and Fe(II) complexes, which may be the only related systems possessing H,H *trans* on distinguishable octahedral faces.

We have independently observed that isomer **16**, the stereochemistry of which is again assigned on the basis of NMR, is the sole product formed initially on treatment of the five-coordinate hydrochloride **9** with LiAlH_4 under CO but that it subsequently undergoes slow thermal rearrangement to yield a mixture containing **14,14'** in an identical ratio (*ca.* 1:3, Figure 2) to that obtained from **10,11**. Formation of a mixture of dihydrido complexes (**14–16**) from the latter, including all three possible *mer*-biPSi isomers, Scheme 1, together with the facile diastereoisomerization of **16**, may be accounted for by intramolecular H,H exchange at octahedral Ir(III), as observed³¹ in the related *cis*-IrH₂(chel)(CO)(PPh_3). The existence of such nonrigidity is further suggested by the observation that the distribution of hydrido(deuterio) isotopomers after treatment of the **10,11** mixture with LiAl^2H_4 showed no evidence for any preferential site occupancy (*syn* vs *anti*) by ^2H (*i.e.*, in the ^1H NMR spectrum, the intensity ratio of hydrogen signals assigned to the mono(deuterio)isotopomers **14a**: **14'a**:**15a**:**16a** is identical with that characteristic of the diastereomer mixture **14–16**, Figure 2).

The long Pt–Cl bond *trans* to Si in **5** is consistent with Cl loss as an activating step in olefin hydroformylation catalyzed by this and related complexes.^{16,34} At 2.44 Å its length exceeds that *trans* to CH_3 (2.41 Å) or H (2.42 Å) in the nonchelate complexes *trans*-Pt(PPh_2R)₂(Y)Cl (Y = R = Me³⁵ or³⁶ Y = H, R = Et), a sequence that follows the progression of Ir–P distances in the complex¹³ IrH(PMe_3)₃(CH_3)(SiEt₃), *i.e.*, 2.30, 2.34, and 2.36 Å *trans* to CH_3 , H, and SiEt₃, respectively. The Ir–Si bond in the 16-electron, five-coordinate complex **9** is, like that¹ in Ir(chel)₂Cl, conspicuously shorter than those in

(33) See: Heinekey, D. M.; Hinkle, A. S.; Close, J. D. *J. Am. Chem. Soc.* **1996**, *117*, 5353. Two-bond H–H coupling has rarely been observed in *cis* dihydrido complexes because the two H atoms are most commonly chemically equivalent (see also refs 9 and 31 for examples where this is not so); corresponding data for related *trans* dihydrido complexes remain exceedingly rare.

(34) Anderson, G. K.; Clark, H. C.; Davies, J. A. *Inorg. Chem.* **1983**, *22*, 427, 434.

(35) Bennett, M. A.; Clark, P. W.; Robertson, G. B.; Whimp, P. O. *J. Organomet. Chem.* **1973**, *63*, C15.

(36) Eisenberg, R.; Ibers, J. A. *Inorg. Chem.* **1965**, *4*, 773.

(32) Meek, D. W.; Tau, K. D. *Inorg. Chem.* **1979**, *17*, 3574.

octahedral 18-electron analogues (Table 4). The short Ir–Cl bond in the same compound is characteristic¹ of a dist-TBP structure²¹ in which the Cl ligand is not brought into a directly *trans* relationship with either H or Si. The Si–Ir–Cl angle is, at 127°, close to the smaller of the two angles H–Ir–Cl (131° and 156°) in the solid state structure^{21b} (neutron diffraction) of IrH₂(PPh^tBu₂)₂Cl. In this latter complex, the hydride distinguished in the slow-limit ¹H NMR spectrum (–100 °C) as pseudo-*trans*³⁷ to Cl is assigned at δ –20.1, suggesting that with a shift of –22.4 the H position in **9** may be the result of an angle at Ir of only a little less than 156°, *i.e.*, putting Si–Ir–H similar to Si–Ir–Si (86°) in Ir(chel)₂Cl. If the CO group is labilized *trans* to Si in the octahedral compound **18**, its ejection may provide access to a five-coordinate ruthenium(II) monocarbonyl, *i.e.*, another example of a 16-electron, d⁶

configuration²⁸ (isoelectronic with the iridium complex **9**). In particular, unsaturation at such a center coupled with the *cis* disposition of H and CO in **18** suggests that this system will be active as a catalyst for hydroformylation, but before this possibility can be investigated further an efficient route to compounds like **17** or **18** will be required.

Acknowledgment. We thank Auburn University, Imperial Oil Ltd., and the NSERC, Canada, for financial support, Dr. G. W. Bushnell for assistance with the X-ray crystallography, and Drs. R. A. Gossage and A. McAuley for useful discussions.

Supporting Information Available: Text giving additional details of the X-ray study, figures giving additional ORTEP views, and tables giving crystal data, positional and thermal parameters, and bond distances and angles for **5**, **9**, **13**, and **19** (33 pages). Ordering information is given on any current masthead page.

OM970518K

(37) Hauger, B. E.; Gusev, D.; Caulton, K. G. *J. Am. Chem. Soc.* **1994**, *116*, 208.